Peer-reviewed version available at Chemosensors 2018, 6, 34; doi:10.3390/chemosensors6030034

Article

Nanoporous Silica-Dye Microspheres for Enhanced Colorimetric Detection of Cyclohexanone

Zheng Li*

Department of Chemical and Biomolecular Engineering, North Carolina State University, 911 Partner Way, Campus Box 7905, Raleigh, NC 27695, USA

* Correspondence: zli47@ncsu.edu; Tel.: +1-217-418-9162

Abstract: Forensic detection of non-volatile nitro explosives poses a tough analytical challenge. A colorimetric sensor comprising ultrasonically prepared silica-dye microspheres was developed for sensitive gas detection of cyclohexanone, a volatile marker of explosives 1,3,5-trinitro-1,3,5-triazinane (RDX) and 1,3,5,7-tetranitro-1,3,5,7-tetrazocane (HMX). The silica-dye composites were synthesized from the hydrolysis of ultrasonically sprayed organosiloxanes under mildly heating conditions (150 °C), which yields microspherical, nanoporous structures with high surface area (~300 m^2/g) for gas exposure. The sensor inks were deposited on cellulose paper and gave sensitive colorimetric responses to trace amount of cyclohexanone vapors even at sub-ppm levels, with the detection limit down to ~150 ppb. The sensor showed high chemical specificity towards cyclohexanone against humidity and other classes of common solvents, including ethanol, acetonitrile, ether, ethyl acetate, and ammonia. Paper-based colorimetric sensors with hierarchical nanostructures could represent an alternative sensing materials for practical applications in the detection of explosives.

Keywords: silica-dye microspheres; hierarchical nanostructure; colorimetric sensing; gaseous cyclohexanone; ppb detection; explosive screening

1. Introduction

Today, there still remains a difficult scientific challenge in the accurate detection and identification of explosives and chemical or biological agents at trace amounts [1]. Sensitivity, specificity, reproducibility, ease of handling, environmental tolerance, and cost are all important factors that ought to be taken into account in the development of useful gas detectors for explosives [2]. Among so many energetic materials, 1,3,5-trinitro-1,3,5-triazinane (RDX) and 1,3,5,7-tetranitro-1,3,5,7-tetrazocane (HMX) are two typical nitro-explosives that are widely used by terrorists and therefore pose a great threat to the civilian and military security [3,4]. However, it is rather difficult to detect either RDX or HMX in the gas phase due to its extremely low volatility, with the saturated vapor pressure of only 10 ppt at ambient conditions. An alternative approach for indirect identification of nitro explosives is to target more volatile but non-energetic species introduced during their manufacturing, e.g. cyclohexanone, a common solvent used for the recrystallization of RDX or HMX [5,6]. Cyclohexanone has a significantly high vapor pressure of ~6500 ppm at 20 °C, thus becoming well-suited to act as a vapor signature for explosive sensing.

In the past decade, a large number of analytical methods for trace explosive screening have been investigated, including GC-MS [7-10], electronic noses [11-14], ion mobility spectrometry [5,15-18], surface acoustic wave devices [19-21] and fluorimetry [22-25]. Some effective approaches, such as solid-phase microextraction (SPME) [26-28], have been extensively explored for ultrasensitive gaseous detection of non-volatile explosives at ppb or ppt level. Many of those techniques, however, suffer from at least one of the following drawbacks: lack of portability, time-consuming sample preparation, demands in sophisticated instrumentation or highly trained personnel for operation and data acquisition [28,29].

Peer-reviewed version available at Chemosensors 2018, 6, 34; doi:10.3390/chemosensors6030034

We described in this work a new method that encapsulates a ketone-sensitive colorimetric indicator, pararosaniline, in the recently reported silica microspheres [30] for sensitive detection of trace level of cyclohexanone vapors. The sensor materials were made from the hydrolysis of siloxane monomers under mildly heating and ultrasonic conditions, which leads to the formation of nanoporous, organically modified silica microspheres, with an averaged diameter of ~500 nm. The as-synthesized inks were pin-printed on the cellulose paper and solidified with the evaporation of solvents prior to the measurements on an ordinary flatbed scanner. The silica-dye composite sensor is optically responsive to cyclohexanone but insensitive to humidity or other common solvents found in explosives including ethanol, acetonitrile, ether, amine and ester. The sensors show greatly improved sensitivity to cyclohexanone that can reach as low as ~150 ppb, 4 times higher than those made from the bulk plasticized films or amorphous sol–gel suspensions. This ultrasonic synthesis provided a scalable and continuous approach for the preparation of such porous materials with hierarchical nanostructures for gas sensing applications.

2. Experimental Methods

2.1. Reagents and Materials.

All chemical reagents, including tetraethoxysilane (TEOS), ethyltriethoxysilane (ETES), pararosaniline, hydrochloric acid, ethanol, polyethylene glycol and other solvents were analytical-reagent grade and used as received unless otherwise specified.

2.2. Preparation of Silica-Dye Composite Microspheres.

The synthesis of silica-dye composite microspheres using a continuous ultrasonic setup is shown in Figure 1: TEOS (0.01 mol) and ethyltriethoxysilanes (0.02 mol) were mixed with ethanol (13 mL), nanopure water (26 mL), and aqueous HCl (1 mL, 0.1 M) plus the ketone-responsive indicator, pararosaniline (100 mg). The precursor solution was introduced into a glass cell and nebulized by a home-made ultrasonic humidifier working at ~10 W/cm^2. The resulting aerosol was carried by an N_2 gas through a tube furnace at a mild heating temperature of 150–300 °C to ensure the optimal porosity of the microspheres; the N_2 gas flow was set at 1.0 SLPM (standard liters per minute). The product was collected in a couple of connected bubblers containing 1:1 v/v mixture of nanopure water and ethanol, then centrifuged and washed with the same solvents three times to remove uncaptured indicators. The final product was redispersed in 9:1 mixtures of ethanol and polyethylene glycol (Mw ≈ 10000) prior to sensor printing.

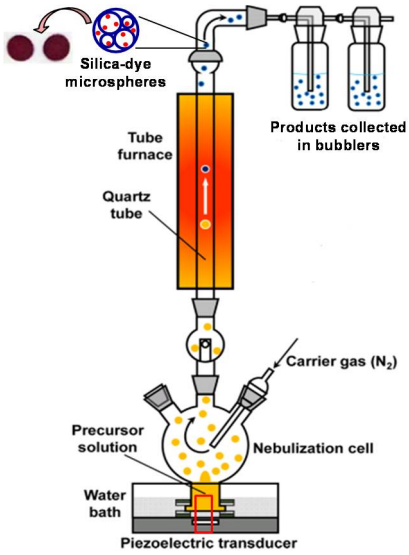

Figure 1. Ultrasonic spray synthesis of the porous silica-dye composite microspheres.

Peer-reviewed version available at Chemosensors 2018, 6, 34; doi:10.3390/chemosensors6030034

2.3. Material Characterization.

For characterization of silica-dye microspheres, powder XRD patterns were obtained on a Siemens−Bruker D-5000 XRD instrument using Cu Kα radiation (wavelength 1.5418 Å) operated at 40 kV and 30 mA. SEM was carried out using a Hitachi S-4700 operated at 10 kV. TEM was performed using a JEOL 2000FX with an acceleration voltage of 200 kV. The Brunauer−Emmett−Teller (BET) specific surface areas were measured by a Quantachrome NOVA 2200e system.

2.4. Preparation of the Paper-Based Sensor.

The colorimetric sensor was deposited on nitrocellulose paper (Whatman) with a robotic pin printer as described in details in previous literature [31-33], which delivered nanoporous inks with silica-dye microspheres encapsulating a ketone-responsive indicator, pararosaniline. After printing, the sensor was dried under vacuum for 1 h at room temperature and stored in N_2 atmosphere for at least 24 h before any measurements.

2.5. Measurement of Gaseous Cyclohexanone.

Analyte flow streams were produced by bubbling dry N_2 through the liquid cyclohexanone. The resulting saturated vapors were then mixed with a diluting stream of dry and wet N_2 to attain the desired concentrations between 0.1 and 100 ppm at 50% relative humidity (RH) using MKS digital mass flow controllers (MFCs). The flow rate was kept at 0.5 SLPM for all the experiments performed in this work. Sensor responses were collected on an Epson Perfection V600 flatbed scanner: sensors were equilibrated with 50% RH nitrogen for 1 min to capture the before-exposure image, and after-exposure image was acquired after 2 min exposure to cyclohexanone vapor.

2.6. Data Analysis.

Colorimetric response of each sensor element was calculated from the differences in red, green, and blue (ΔRGB) values by comparing before- to after-exposure images using the software ImageJ. For visualization purposes only, color difference RGB values were expanded from 3 bits (i.e., 3–10) to 8 bits (i.e., 0–255). For the measurement of the control or each concentration of cyclohexanone, quintuplicate trials were collected. S/N was calculated from the Euclidean distance (ED, i.e. the square root of the sum of square of RGB channels) and incorporated in the final database for statistical analysis, in which the signals were defined as the difference between the response of certain concentration of cyclohexanone and that of the averaged control, and noise was defined as the standard deviation among quintuplicate trials of the control for ED of each spot, namely

$$S = ED_{cyclohexanone-k} - ED_{control-avg};\ N = \sum_{k=1}^{n} \left(ED_{control-k} - ED_{control-avg}\right)^2 / (n-1)$$

3. Results and Discussions

3.1. Silica-Dye Composite Microspheres.

Factors that reflect the performance of optical gas sensors, such as response time, sensitivity, reproducibility, selectivity, susceptibility to interferents, can be heavily influenced by the choice of substrates or matrices of the colorants [34-36]. Porous organosilica materials [37-39] provide impressive physical and chemical properties including high stability, tunable porosity or hydrophobicity, and ease of modification, which can be promisingly selected as sensor media to ensure the robust encapsulation and solvation of chemical dyes, high contact area for gas exposure, as well as prevention from dye leaching. Porous silica matrices as host materials can impressively enhance overall sensitivity of chemo-responsive dyes for gaseous or aqueous detection of relevant analytes of interest.

Ultrasonic spray pyrolysis (USP) [40-42] is a tunable and scalable approach for the preparation of a wide variety of hierarchical materials, including porous carbons, transition metal oxides or

chalcogenides, metallic nanoparticles, polymers, etc. USP is also well suited for the continuous synthesis of organosilica particles, in large part with microspherical geometries. In a typical USP process, ultrasound is used to nebulize precursor solution droplets dispersed in an inert carrier gas (Ar or N_2, Figure 1). With the pyrolysis of aerosol droplets in the furnace, evaporation of solvents and reactions between precursors occur, so as to generate microscale or nanoscale solid products with spherical morphologies. Using low-volatility precursors, the reactions responsible for the formation of products are confined within each individual droplet. The droplets formed in this matter can serve as individual chemical microreactors that impose morphology control on the products.

Choices of siloxane precursors and reaction temperatures used in ultrasonic synthesis can largely affect the morphology of microspheres [43,44]. To that end, we employed a mixture of TEOS and ETES (1:2 molar ratio) as the precursor to guarantee the optimal permeability and porosity of the as-synthesized silica-dye composites. A ketone-responsive indicator, pararosaniline, was incorporated in the precursor for the ultrasonic spray synthesis. The aerosol-gel reaction was kept at either 150 or 300 °C to investigate the impact of the temperature on morphologies of the products. Electron microscopy graphs reveal that hollow and more porous microspheres (520 ± 50 nm in diameter) with smoother surfaces were obtained at 150 °C (Figures 2a), while those micron-scale particles tend to become more solid and compact (440 ± 60 nm in diameter) as the temperature goes up to 300 °C (Figure 2b). Powder XRD spectrum shows amorphous polymeric structure of both microspheres, as indicated by the characteristic broad peaks at 25° and 40° (Figure S1).

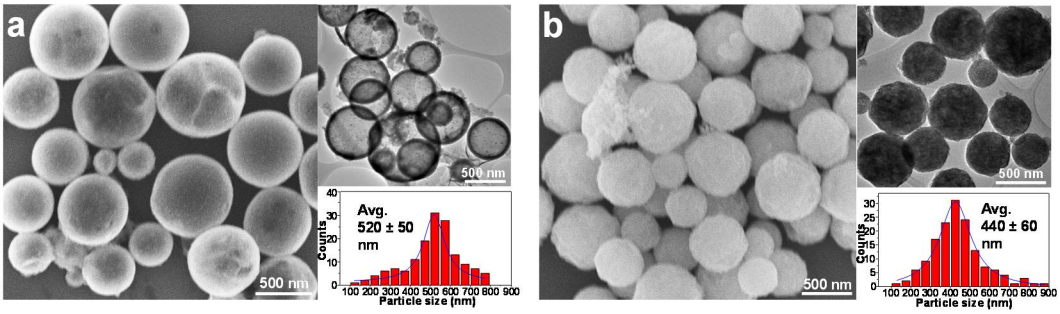

Figure 2. Morphologies of Silica-dye microspheres synthesized at (a) 150 °C and (b) 300 °C, with the particle size of 520 ± 50 nm and 440 ± 60 nm, respectively.

3.2. Sensor Responses of Gaseous Cyclohexanone.

Colorimetric inks made of silica-dye microspheres were pin-printed on a nitrocellulose paper and dried out for the detection of target vapors, which is generated from the saturated vapor of liquid cyclohexanone. The designed sensing mechanism are based on nucleophilic addition by the three equivalent amino groups of the dye to the carbonyl moriety of cyclohexanone in the formation of an imine species [45-48], leading to changes in UV-vis absorption band that allows for direct identification of low or high concentration by the naked eye (Figure 3).

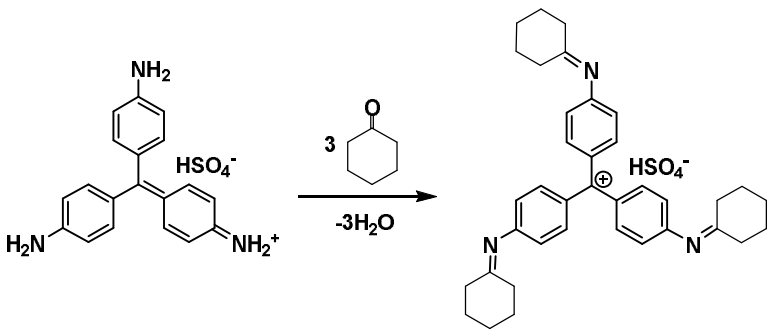

Figure 3. Colorimetric detection mechanism of cyclohexanone using an amine-based indicator, pararosaniline, in the formation of an imine product.

We have proven in the previous research that the colorimetric reactions of typical indicators with gas analytes using porous matrices can reach equilibrated responses within 1 or 2 min [33,49]. The sensor element essentially has a fast response time (i.e., to reach 50% of saturated response in the first 30 s of exposure) and once equilibrated, the overall response is independent of flow rates or doses. Therefore, we collected sensor responses to different concentrations of cyclohexanone after 2 min exposure, as shown in Figure 4. Significant color changes from red (color of the initial dye) to dark red (color of the product after exposure) were observed for the target molecule at ppm and even sub-ppm levels. Sensor responses become rather strong at gas concentrations above 1 ppm, while slightly color changes can still be discerned in the range of 0.1–0.25 ppm. The left sensor element made from 150 °C silica microsphere suspensions is generally more reactive than the right one prepared at 300 °C for each concentration, which is consistent with the magnitude of the surface areas of two nanoporous inks: silica microspheres synthesized at 150 or 300 °C give BET specific surface areas of 288 or 179 m^2/g, respectively (Figure 5a and 5b); higher surface area of the 150 °C silica microsphere facilitates the gas exposure of dye molecules, and therefore results in enhanced responsiveness to the carbonyl compound.

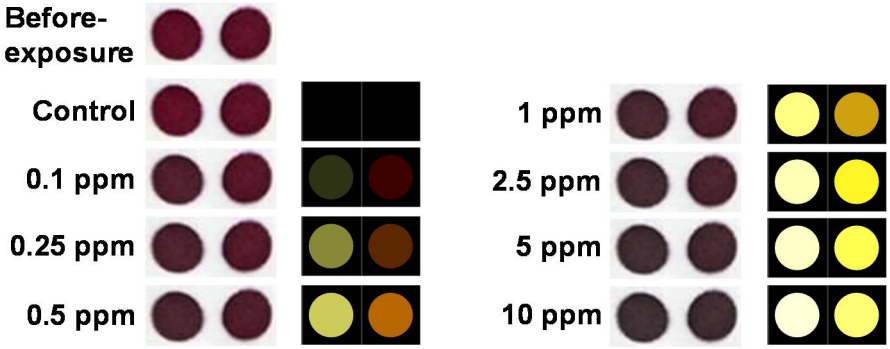

Figure 4. Images of sensors made from 150 (left spot) and 300 °C (right spot) microspheres before and after the vapor exposure, and RGB color different profiles (right) that show colorimetric sensor responses to different concentrations of cyclohexanone plus a control (i.e., N_2) for 2 min. Each pattern was averaged out of three trials. For display purposes, each RGB profile was narrowed down from 8 bit (0-255) to 3 bit (3-10) color range.

3.3. Discussions: Influence of Nanostructure on Sensing Properties.

The development of chemical sensing platforms has increasingly employed substrates fabricated with advanced processing techniques; their overall morphologies, especially some microstructures or nanostructures, must be fully characterized in order to gain a comprehensive insight into the sensing mechanisms. The high-resolution TEM (HR-TEM) micrographs demonstrate the highly hierarchical structure of the microspheres synthesized at 150 °C, from which we can observe a substantial number of nanopores incorporated in the microsphere (1–2 nm in diameter, Figure 6a). The hierarchically nanoscale features of the microsphere contribute to their improved surface area and consequently enhanced gas sensing properties. However, materials obtained at higher temperature show no significant nanopores, thus giving reduced porosity and reactivity to gaseous analytes (Figure 6b). This observation is consistent with the pore size distributions of both microspheres according to the Barrett-Joyner-Halenda (BJH) model [50] (Figure 5c and 5d).

The porosity of any sensing materials has profound impacts on both the accessibility of analyte molecules to receptors and the ability to immobilize or encapsulate chemical dyes. Based on the appearance of materials obtained under different synthetic conditions, we propose a mechanism for the formation of products as shown Figure S2: higher temperature condition tends to trigger a homogeneous process for hydrolysis of siloxane precursors and the following pyrolysis yields contracted microspheres with collapsed surface pores, diminishing both particle size and porosity; at lower temperature, however, the mixture solution undergoes a phase separation between H_2O

Peer-reviewed version available at Chemosensors 2018, 6, 34; doi:10.3390/chemosensors6030034

and immiscible siloxane precursors, and hydrolysis is more likely to occur at the aqueous–organic interfaces, which leads to hollow microspheres with well-defined hierarchical nanostructure. The latter remarkably improves the permeability and accessibility of gaseous analytes to the encapsulated dye molecules in the organosilica hosts and is preferable to be used in the gas sensing applications.

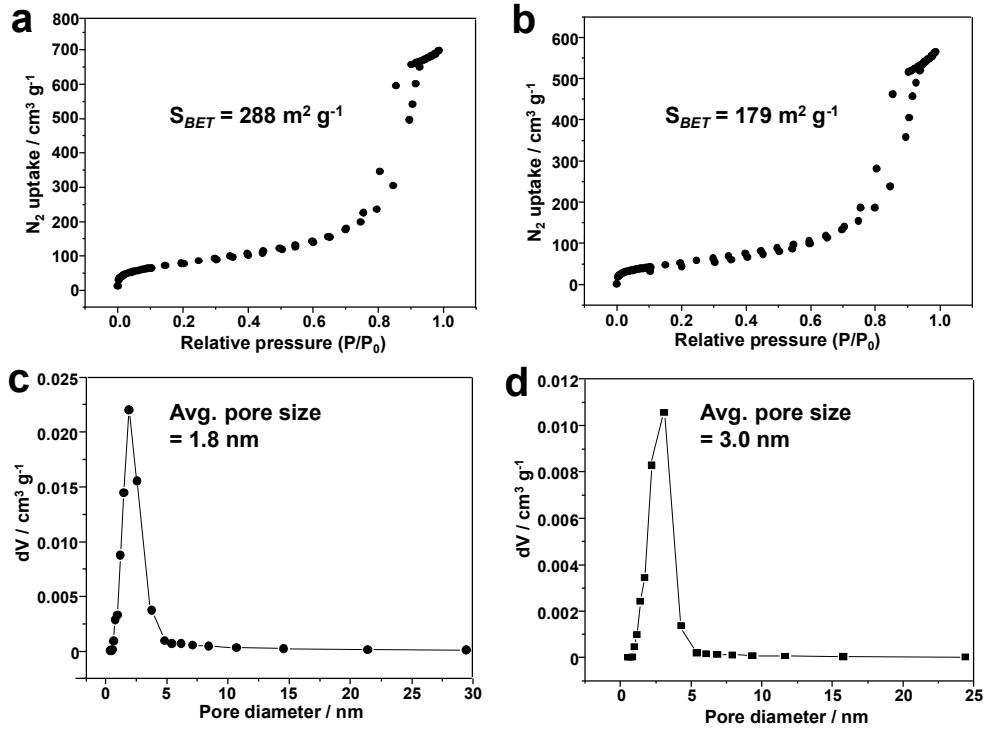

Figure 5. Gas adsorption experiments of two microspheres. (a) and (b), N_2 adsorption isotherms of two microspheres prepared at 150 and 300 °C, respectively; (c) and (d), pore size distributions of two microspheres based on BJH model. All measurements were performed with N_2 at 78 K.

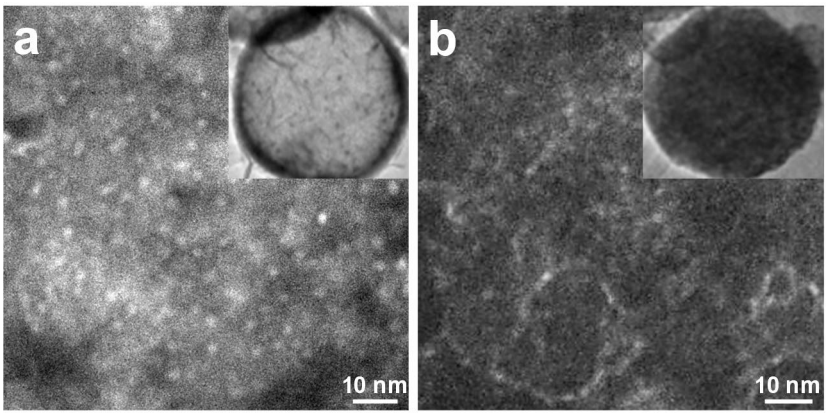

Figure 6. HR-TEM micrographs of microspheres synthesized at (a) 150 °C and (b) 300 °C. Hierarchical structure with nanopores is present in graph (a).

3.4. Limit of Detection and Specificity.

As an approach for quantitative determination of cyclohexanone, the response curve of the more responsive sensor (i.e., microspheres obtained at 150 °C) is plotted to demonstrate the correlation of sensor responses as a function of the concentration (Figure 7). The calibration curve shows good linearity in the low concentration range of 0.1–2.5 ppm, from which we can calculate the limit of detection (LOD) by extrapolating the curve to the concentration where the signal is

Peer-reviewed version available at Chemosensors 2018, 6, 34; doi:10.3390/chemosensors6030034

equal to three times as much as the noise (i.e., S/N = 3). An estimated LOD of ~0.15 ppm was achieved based on 2 min exposure, which is well below the vapor pressure of cyclohexanone, or ~6500 ppm at 20 °C.

The paper-based colorimetric sensor strip reported herein is ideal for rapid headspace inspection of unknown samples in the field and superior to prior studies on cyclohexanone detection in terms of the sensitivity. In comparison with the functionalized single-walled carbon nanotube (SWCNT)-based chemiresistors developed by Swager *et al.* [51] for similar applications, the current method is able to substantially improve LOD from 5 ppm to low sub-ppm level by slightly elongating the exposure time from 30 s to 2 min. Compared to our recent results on optical cyclohexanone sensing using the same colorimetric probe but different host matrices (i.e., plasticized films, with neither significant microscale structure nor comparable surface areas), sensor response from organosilica microspheres is generally 30–50% higher for each concentration, and the reported sensitivity in current work is enhanced by 4–5 times (0.15 ppm vs. 0.84 ppm) [52]. This demonstrates the primary role of the hierarchical nanostructure in improving optical properties of sensing materials.

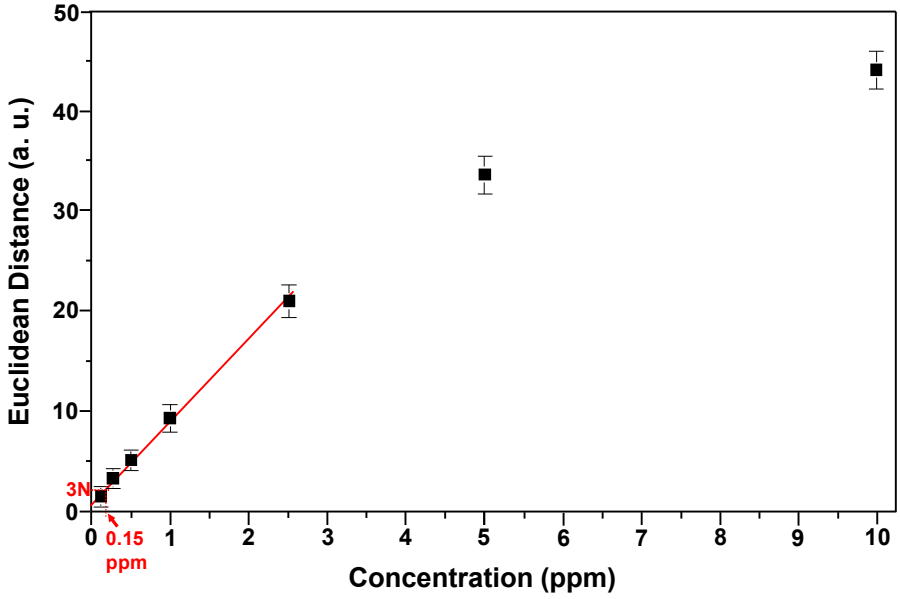

Figure 7. The calculation of the limit of detection of cyclohexanone. Data points between 0.1 and 2.5 ppm were linearly fitted and extrapolated to the concentration when S/N =3. The LOD is estimated to be ~0.15 ppm.

Measurements on various interferents with or without the presence of real analytes were performed to demonstrate the chemical selectivity of the developed optical sensor. We first observed very little response in the sensor to changes in humidity (Figure S3): sensor response is nearly at the same level as the controls for exposure of 1 ppm cyclohexanone at relative humidity (RH) ranging from 10–90%. This is in large part due to the use of hydrophobic formulations to prevent the potential contact of water molecules with sensor elements. We further tested the sensor against a series of organic solvents that can be commonly found in the household environment or during the manufacturing of explosives. The sensor is designed to primarily probe the electrophilic property of targeted ketone species, and so it ought to be less responsive to other classes of volatile organic compounds. In accord with the expectation, the sensor exhibits ideal chemical specificity toward cyclohexanone: very tiny response is observed for exposure of ethanol, acetonitrile, ether, ammonia and ethyl acetate (Figure 8). Tests of potential interferents illustrate the possible applications of the developed sensor for field screening of explosives that could contain trace amount of cyclohexanone as characteristic impurities.

Peer-reviewed version available at Chemosensors 2018, 6, 34; doi:10.3390/chemosensors6030034

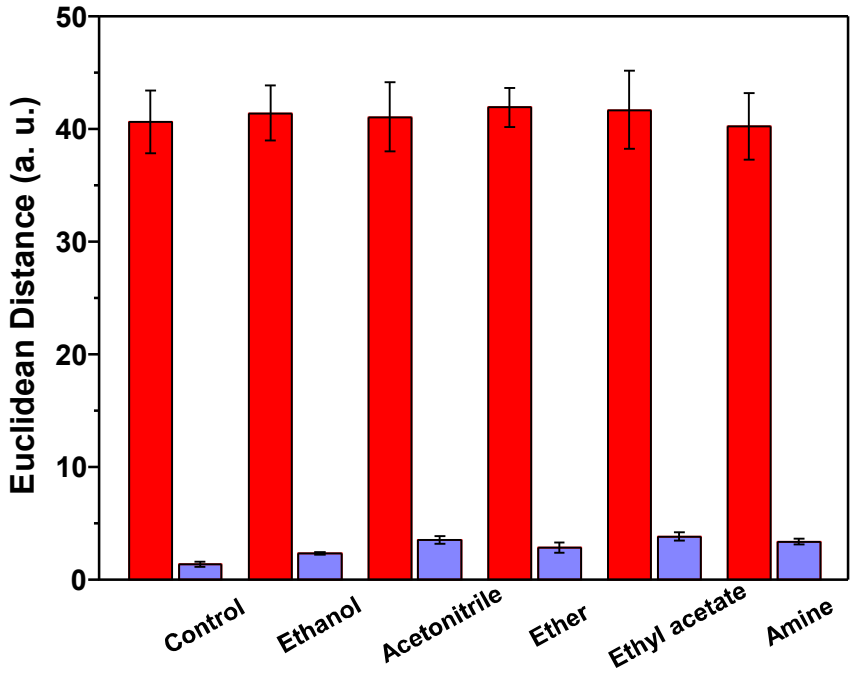

Figure 7. Sensor responses to 1 ppm cyclohexanone with (red bars) or without (blue bars) the presence of interferents. Error bars showing the standard deviation among three replicates of each analyte are displayed.

5. Conclusions

A new method that encapsulates a chemo-responsive dye in highly porous organosilica matrices was reported for sensitive colorimetric detection of trace amount of cyclohexanone, a volatile explosive indicator from nitro-compounds such as RDX and HMX. Using ultrasonic and aerosol-gel synthesis, hierarchically nanoporous microspheres were produced at relatively low temperature as colorimetric sensor inks. Silica-dye composite microspheres have an averaged diameter of ~500 nm, with the size of nanopores around 1–2 nm. The paper-based colorimetric sensor strip allowed for quick quantification of gaseous cyclohexanone in 2 min, with the detection limit down to ~150 ppb. The silica-dye composite sensor is optically responsive to cyclohexanone but insensitive to common interferents involved in the production of nitro-explosives, including humidity, ethanol, acetonitrile, ether, ester and amine. The continuous and scalable ultrasonic spray synthesis provides a facile approach to prepare porous materials with hierarchical nanostructures for ultrasensitive detection of gas analytes. This method has significant implications in the detection and identification of non-volatile nitro-explosives via the recognition of signature molecules from the headspace gas, and may pave a path for developing a useful complement to other available sensing technologies used in security checks and forensic assessment of improvised explosives.

Supplementary Materials: The following are available online at www.mdpi.com/xxx/s1, Figure S1: Powder XRD patterns of two silica-dye microspheres synthesized at 150 and 300 °C. The spectra confirm the amorphous structures of both microspheres. Figure S2: Proposed mechanisms showing the formation of porous microspheres at (a) 150 and (b) 300 °C. Figure S3: Humidity tests of microsphere-based sensors synthesized at 150 °C. (a) Before- and after-exposure images of the sensor spot and RBG difference profiles upon exposure of 1 ppm cyclohexanone with the 10%–90% relative humidity (RH), which is displayed in the color range of 3–10. (b) Sensor response to 1 ppm cyclohexanone at different levels of RH.

Author Contributions: Z. L. solely came up with the idea, performed all the experiments and wrote the manuscript.

Acknowledgments: Z. L. acknowledges the postdoctoral financial support from the Procter & Gamble Foundation (085310). This work was carried out in part in the Frederick Seitz Materials Research Laboratory

Central Facilities at the University of Illinois and the Analytical Instrumentation Facility (AIF) at the North Carolina State University.

Conflicts of Interest: The author declares no conflict of interest.

References

1. Yinon, J. *Counterterrorist detection techniques of explosives*. Elsevier B. V.: Amsterdam, 2007.
2. Strobbia, P.; Odion, R.; Vo-Dinh, T. Spectroscopic chemical sensing and imaging: From plants to animals and humans. *Chemosensors* **2018**, *6*, 11.
3. Long, Y.; Chen, J. Systematic study of the reaction kinetics for hmx. *J. Phys. Chem. A* **2015**, *119*, 4073-4082.
4. Chatterjee, S.; Deb, U.; Datta, S.; Walther, C.; Gupta, D.K. Common explosives (tnt, rdx, hmx) and their fate in the environment: Emphasizing bioremediation. *Chemosphere* **2017**, *184*, 438-451.
5. Lai, H.; Leung, A.; Magee, M.; Almirall, J.R. Identification of volatile chemical signatures from plastic explosives by spme-gc/ms and detection by ion mobility spectrometry. *Anal. Bioanal. Chem.* **2010**, *396*, 2997-3007.
6. Chen, G.; Xia, M.; Lei, W.; Wang, F.; Gong, X. Prediction of crystal morphology of cyclotrimethylene trinitramine in the solvent medium by computer simulation: A case of cyclohexanone solvent. *J. Phys. Chem. A* **2014**, *118*, 11471-11478.
7. Ong, T.-H.; Mendum, T.; Geurtsen, G.; Kelley, J.; Ostrinskaya, A.; Kunz, R. Use of mass spectrometric vapor analysis to improve canine explosive detection efficiency. *Anal. Chem.* **2017**, *89*, 6482-6490.
8. Rahman, M.M.; Jiang, T.; Tang, Y.; Xu, W. A simple desorption atmospheric pressure chemical ionization method for enhanced non-volatile sample analysis. *Anal. Chim. Acta* **2018**, *1002*, 62-69.
9. Zamora, D.; Amo-Gonzalez, M.; Lanza, M.; Fernández de la Mora, G.; Fernández de la Mora, J. Reaching a vapor sensitivity of 0.01 parts per quadrillion in the screening of large volume freight. *Anal. Chem.* **2018**, *90*, 2468-2474.
10. Stefanuto, P.-H.; Perrault, K.; Focant, J.-F.; Forbes, S. Fast chromatographic method for explosive profiling. *Chromatography* **2015**, *2*, 213.
11. Strle, D.; Štefane, B.; Trifkovič, M.; Van Miden, M.; Kvasić, I.; Zupanič, E.; Muševič, I. Chemical selectivity and sensitivity of a 16-channel electronic nose for trace vapour detection. *Sensors* **2017**, *17*, 2845.
12. Patil, S.J.; Duragkar, N.; Rao, V.R. An ultra-sensitive piezoresistive polymer nano-composite microcantilever sensor electronic nose platform for explosive vapor detection. *Sens. Actuators B* **2014**, *192*, 444-451.
13. Li, Z.; Bassett, W.P.; Askim, J.R.; Suslick, K.S. Differentiation among peroxide explosives with an optoelectronic nose. *Chem. Commun.* **2015**, *51*, 15312-15315.
14. Staymates, M.E.; MacCrehan, W.A.; Staymates, J.L.; Kunz, R.R.; Mendum, T.; Ong, T.-H.; Geurtsen, G.; Gillen, G.J.; Craven, B.A. Biomimetic sniffing improves the detection performance of a 3d printed nose of a dog and a commercial trace vapor detector. *Sci. Rep.* **2016**, *6*, 36876.
15. Roscioli, K.M.; Davis, E.; Siems, W.F.; Mariano, A.; Su, W.; Guharay, S.K.; Hill, H.H. Modular ion mobility spectrometer for explosives detection using corona ionization. *Anal. Chem.* **2011**, *83*, 5965-5971.
16. Senesac, L.; Thundat, T.G. Nanosensors for trace explosive detection. *Mater. Today* **2008**, *11*, 28-36.
17. Peng, L.; Hua, L.; Wang, W.; Zhou, Q.; Li, H. On-site rapid detection of trace non-volatile inorganic explosives by stand-alone ion mobility spectrometry via acid-enhanced evaporization. *Sci. Rep.* **2014**, *4*, 6631.
18. Choi, S.-S.; Son, C.E. Analytical method for the estimation of transfer and detection efficiencies of solid state explosives using ion mobility spectrometry and smear matrix. *Anal. Methods* **2017**, *9*, 2505-2510.
19. Mujahid, A.; Dickert, F. Surface acoustic wave (saw) for chemical sensing applications of recognition layers. *Sensors* **2017**, *17*, 2716.
20. Gupta, D.; Chen, X.; Wang, C.-C.; Trivedi, S.; Choa, F.-S. Stand-off chemical detection using photoacoustic sensing techniques—from single element to phase array. *Chemosensors* **2018**, *6*, 6.
21. Nimal, A.T.; Mittal, U.; Singh, M.; Khaneja, M.; Kannan, G.K.; Kapoor, J.C.; Dubey, V.; Gutch, P.K.; Lal, G.; Vyas, K.D., *et al.* Development of handheld saw vapor sensors for explosives and cw agents. *Sens. Actuators B* **2009**, *135*, 399-410.
22. García-Calvo, J.; Calvo-Gredilla, P.; Ibáñez-Llorente, M.; Romero, D.C.; Cuevas, J.V.; García-Herbosa, G.; Avella, M.; Torroba, T. Surface functionalized silica nanoparticles for the off–on fluorogenic detection of an improvised explosive, tatp, in a vapour flow. *J. Mater. Chem. A* **2018**, *6*, 4416-4423.

23. Chen, H.-Y.; Ruan, L.-W.; Jiang, X.; Qiu, L.-G. Trace detection of nitro aromatic explosives by highly fluorescent g-c3n4 nanosheets. *Analyst* **2015**, *140*, 637-643.
24. Peng, X.; Liu, H.; Liu, A.; Xu, W.; Fu, Y.; He, Q.; Cao, H.; Cheng, J. Ultrasensitive and direct fluorescence detection of rdx explosive vapor via side-chain terminal functionalization of a polyfluorene probe. *Anal. Methods* **2018**, *10*, 1695-1702.
25. Wang, C.; Huang, H.; Bunes, B.R.; Wu, N.; Xu, M.; Yang, X.; Yu, L.; Zang, L. Trace detection of rdx, hmx and petn explosives using a fluorescence spot sensor. *Sci. Rep.* **2016**, *6*, 25015.
26. Gaurav; Malik, A.K.; Rai, P.K. Development of a new spme–hplc–uv method for the analysis of nitro explosives on reverse phase amide column and application to analysis of aqueous samples. *J. Hazard. Mater.* **2009**, *172*, 1652-1658.
27. Bianchi, F.; Bedini, A.; Riboni, N.; Pinalli, R.; Gregori, A.; Sidisky, L.; Dalcanale, E.; Careri, M. Cavitand-based solid-phase microextraction coating for the selective detection of nitroaromatic explosives in air and soil. *Anal. Chem.* **2014**, *86*, 10646-10652.
28. McEneff, G.L.; Murphy, B.; Webb, T.; Wood, D.; Irlam, R.; Mills, J.; Green, D.; Barron, L.P. Sorbent film-coated passive samplers for explosives vapour detection part a: Materials optimisation and integration with analytical technologies. *Sci. Rep.* **2018**, *8*, 5815.
29. Albert, K.J.; Lewis, N.S.; Schauer, C.L.; Sotzing, G.A.; Stitzel, S.E.; Vaid, T.P.; Walt, D.R. Cross-reactive chemical sensor arrays. *Chem. Rev.* **2000**, *100*, 2595-2626.
30. Li, Z.; Suslick, K.S. Ultrasonic preparation of porous silica-dye microspheres: Sensors for quantification of urinary trimethylamine n-oxide. *ACS Appl. Mater. Interfaces* **2018**, *10*, 15820-15828.
31. Askim, J.R.; Li, Z.; LaGasse, M.K.; Rankin, J.M.; Suslick, K.S. An optoelectronic nose for identification of explosives. *Chem. Sci.* **2016**, *7*, 199-206.
32. Li, Z.; Li, H.; LaGasse, M.K.; Suslick, K.S. Rapid quantification of trimethylamine. *Anal. Chem.* **2016**, *88*, 5615-5620.
33. Li, Z.; Jang, M.; Askim, J.R.; Suslick, K.S. Identification of accelerants, fuels and post-combustion residues using a colorimetric sensor array. *Analyst* **2015**, *140*, 5929-5935.
34. Nery, E.W.; Kubota, L.T. Sensing approaches on paper-based devices: A review. *Anal. Bioanal. Chem.* **2013**, *405*, 7573-7595.
35. Li, Z.; Suslick, K.S. Portable optoelectronic nose for monitoring meat freshness. *ACS Sens.* **2016**, *1*, 1330-1335.
36. Khodasevych, I.; Parmar, S.; Troynikov, O. Flexible sensors for pressure therapy: Effect of substrate curvature and stiffness on sensor performance. *Sensors* **2017**, *17*, 2399.
37. Burleigh, M.C.; Markowitz, M.A.; Spector, M.S.; Gaber, B.P. Porous organosilicas: An acid-catalyzed approach. *Langmuir* **2001**, *17*, 7923-7928.
38. Ma, M.; Yan, F.; Yao, M.; Wei, Z.; Zhou, D.; Yao, H.; Zheng, H.; Chen, H.; Shi, J. Template-free synthesis of hollow/porous organosilica–fe3o4 hybrid nanocapsules toward magnetic resonance imaging-guided high-intensity focused ultrasound therapy. *ACS Appl. Mater. Interfaces* **2016**, *8*, 29986-29996.
39. Du, G.; Peng, J.; Zhang, Y.; Zhang, H.; Lü, J.; Fang, Y. One-step synthesis of hydrophobic multicompartment organosilica microspheres with highly interconnected macro-mesopores for the stabilization of liquid marbles with excellent catalysis. *Langmuir* **2017**, *33*, 5223-5235.
40. Skrabalak, S.E.; Suslick, K.S. Porous mos2 synthesized by ultrasonic spray pyrolysis. *J. Am. Chem. Soc.* **2005**, *127*, 9990-9991.
41. Bang, J.H.; Helmich, R.J.; Suslick, K.S. Nanostructured zns:Ni2+ photocatalysts prepared by ultrasonic spray pyrolysis. *Adv. Mater.* **2008**, *20*, 2599-2603.
42. Xu, H.; Zeiger, B.W.; Suslick, K.S. Sonochemical synthesis of nanomaterials. *Chem. Soc. Rev.* **2013**, *42*, 2555-2567.
43. Jerónimo, P.C.A.; Araújo, A.N.; Conceição B.S.M. Montenegro, M. Optical sensors and biosensors based on sol–gel films. *Talanta* **2007**, *72*, 13-27.
44. Yao, N.; Xiong, G.; Yeung, K.L.; Sheng, S.; He, M.; Yang, W.; Liu, X.; Bao, X. Ultrasonic synthesis of silica−alumina nanomaterials with controlled mesopore distribution without using surfactants. *Langmuir* **2002**, *18*, 4111-4117.
45. Roy, B.; Halder, S.; Guha, A.; Bandyopadhyay, S. Highly selective sub-ppm naked-eye detection of hydrazine with conjugated-1,3-diketo probes: Imaging hydrazine in drosophila larvae. *Anal. Chem.* **2017**, *89*, 10625-10636.

394 46. Xiao, L.; Tu, J.; Sun, S.; Pei, Z.; Pei, Y.; Pang, Y.; Xu, Y. A fluorescent probe for hydrazine and its in vivo
395 applications. *RSC Adv.* **2014**, *4*, 41807-41811.
396 47. Baud, D.; Ladkau, N.; Moody, T.S.; Ward, J.M.; Hailes, H.C. A rapid, sensitive colorimetric assay for the
397 high-throughput screening of transaminases in liquid or solid-phase. *Chem. Commun.* **2015**, *51*,
398 17225-17228.
399 48. Dilek, O.; Bane, S. Turn on fluorescent probes for selective targeting of aldehydes. *Chemosensors* **2016**, *4*, 5.
400 49. Li, Z.; Suslick, K.S. A hand-held optoelectronic nose for the identification of liquors. *ACS Sens.* **2018**, *3*,
401 121-127.
402 50. Barrett, E.P.; Joyner, L.G.; Halenda, P.P. The determination of pore volume and area distributions in
403 porous substances. I. Computations from nitrogen isotherms. *J. Am. Chem. Soc.* **1951**, *73*, 373-380.
404 51. Frazier, K.M.; Swager, T.M. Robust cyclohexanone selective chemiresistors based on single-walled carbon
405 nanotubes. *Anal. Chem.* **2013**, *85*, 7154-7158.
406 52. Li, Z.; Fang, M.; LaGasse, M.K.; Askim, J.R.; Suslick, K.S. Colorimetric recognition of aldehydes and
407 ketones. *Angew. Chem. Int. Ed.* **2017**, *56*, 9860-9863.
408
409